

RESEARCH ARTICLE

An amino-terminal fragment of apolipoprotein E4 leads to behavioral deficits, increased PHF-1 immunoreactivity, and mortality in zebrafish

Madyson M. McCarthy, Makenna J. Hardy, Saylor E. Leising, Alex M. LaFollette, Erica S. Stewart, Amelia S. Cogan, Tanya Sanghal, Katie Matteo, Jonathon C. Reeck, Julia T. Oxford, Troy T. Rohn*

Department of Biological Sciences, Boise State University, Boise, Idaho, United States of America

* trohn@boisestate.edu



OPEN ACCESS

Citation: McCarthy MM, Hardy MJ, Leising SE, LaFollette AM, Stewart ES, Cogan AS, et al. (2022) An amino-terminal fragment of apolipoprotein E4 leads to behavioral deficits, increased PHF-1 immunoreactivity, and mortality in zebrafish. PLoS ONE 17(12): e0271707. <https://doi.org/10.1371/journal.pone.0271707>

Editor: Weidong Le, First Affiliated Hospital of Dalian Medical University, CHINA

Received: July 5, 2022

Accepted: October 19, 2022

Published: December 15, 2022

Peer Review History: PLOS recognizes the benefits of transparency in the peer review process; therefore, we enable the publication of all of the content of peer review and author responses alongside final, published articles. The editorial history of this article is available here: <https://doi.org/10.1371/journal.pone.0271707>

Copyright: © 2022 McCarthy et al. This is an open access article distributed under the terms of the [Creative Commons Attribution License](https://creativecommons.org/licenses/by/4.0/), which permits unrestricted use, distribution, and reproduction in any medium, provided the original author and source are credited.

Data Availability Statement: All relevant data are within the manuscript and its [Supporting Information](#) files.

Abstract

Although the increased risk of developing sporadic Alzheimer's disease (AD) associated with the inheritance of the apolipoprotein E4 (*APOE4*) allele is well characterized, the molecular underpinnings of how ApoE4 imparts risk remains unknown. Enhanced proteolysis of the ApoE4 protein with a toxic-gain of function has been suggested and a 17 kDa amino-terminal ApoE4 fragment (nApoE4₁₋₁₅₁) has been identified in post-mortem human AD frontal cortex sections. Recently, we demonstrated *in vitro*, exogenous treatment of nApoE4₁₋₁₅₁ in BV2 microglial cells leads to uptake, trafficking to the nucleus and increased expression of genes associated with cell toxicity and inflammation. In the present study, we extend these findings to zebrafish (*Danio rerio*), an *in vivo* model system to assess the toxicity of nApoE4₁₋₁₅₁. Exogenous treatment of nApoE4₁₋₁₅₁ to 24-hour post-fertilization for 24 hours resulted in significant mortality. In addition, developmental abnormalities were observed following treatment with nApoE4₁₋₁₅₁ including improper folding of the hindbrain, delay in ear development, deformed yolk sac, enlarged cardiac cavity, and significantly lower heart rates. A similar nApoE3₁₋₁₅₁ fragment that differs by a single amino acid change (C>R) at position 112 had no effects on these parameters under identical treatment conditions. Decreased presence of pigmentation was noted for both nApoE3₁₋₁₅₁- and nApoE4₁₋₁₅₁-treated larvae compared with controls. Behaviorally, touch-evoked responses to stimulus were negatively impacted by treatment with nApoE4₁₋₁₅₁ but did not reach statistical significance. Additionally, triple-labeling confocal microscopy not only confirmed the nuclear localization of the nApoE4₁₋₁₅₁ fragment within neuronal populations following exogenous treatment, but also identified the presence of tau pathology, one of the hallmark features of AD. Collectively, these *in vivo* data demonstrating toxicity as well as sublethal effects on organ and tissue development support a novel pathophysiological function of this AD associated-risk factor.

Funding: This work was funded by the NIH Blueprint for Neuroscience Research 2R15AG042781-03 to Troy T. Rohn. The project described was also supported by Institutional Development Awards (IDeA) from the National Institute of General Medical Sciences of the National Institutes of Health under Grants #P20GM103408 and #P20GM109095, Directorate for Biological Sciences, 0619793, 0923535 to Julia T. Oxford. The funders had no role in study design, data collection and analysis, decision to publish, or preparation of the manuscript.

Competing interests: The authors have declared that no competing interests exist.

Introduction

Alzheimer's disease (AD) is a neurodegenerative disease encompassing the most prevalent form of dementia characterized by amyloid plaques and neurofibrillary tangles (NFTs) [1, 2]. Early-onset AD has been associated with autosomal-dominant mutations in the amyloid precursor gene (APP), presenilin-1 and -2 (PSEN1/PSEN2) genes [2]. These mutations collectively comprising what is known as early-onset AD, affect approximately 5% of all known AD cases [3]. The majority of AD cases are characterized as late-onset in which the greatest risk factors for the disease are environmental (*e.g.*, aging and lifestyle choices) in addition to the inheritance of an apolipoprotein (APOE) allele, namely apolipoprotein E4 (APOE4) [2, 4]. The APOE gene has several isoforms of importance that are affected by a cysteine to arginine polymorphism: APOE2 (C112, C158), APOE3 (C112, R158), and APOE4 (R112, R158) [5, 6]. A carrier of the APOE4 allele increases the risk of developing AD by four- to twelve-fold [2]. However, the mechanisms of how ApoE4 contributes to increased risk of disease have remained elusive.

The APOE gene encodes the main cholesterol transporter protein (ApoE) in the CNS that is taken up by cells primarily through the low-density lipoprotein receptor (LDLR) family [7, 8]. Cholesterol transport in both the periphery and the CNS are vital for basal cellular function, but neurons are in critical need of adequate supply for synaptogenesis and neurite outgrowth [9]. The ApoE isoforms differ in their functional ability through the stepwise change in cysteine (C) to arginine (R) from ApoE2 to ApoE4 as described above [6]. The C112→R112 mutation has the ability to alter the side chain orientation of ApoE4 compared to ApoE2 and ApoE3 through the formation of a salt bridge combining R112 to E109 [6, 9, 10]. Data supports changes in the conformational structure of the isoforms from the C→R substitutions creates an increased likelihood of the generation of toxic fragmentation [11]. The role of ApoE4 proteolysis as a possible mechanism underlying disease risk has been supported by the findings of 17–20 kDa ApoE4 fragments in the prefrontal cortex from post-mortem AD patient tissue that localize within NFTs [11–15].

We recently examined the role of an amino-terminal fragment of ApoE4 previously identified in the human AD brain utilizing cultured BV2 microglia cells. Our findings demonstrated that exogenous application of this amino-terminal fragment of ApoE4 (nApoE4_{1–151}) in microglial cells resulted in uptake of nApoE4_{1–151}, trafficking to microglial nuclei, and the expression of numerous genes associated with inflammation [16–18]. To expand on this work, the current study employed an *in vivo* zebrafish system to study the fragment in a complex organism. The zebrafish model system has increasingly been used to study neurodegenerative diseases in vertebrates [19–21]. Some of the many benefits to this model are the rapid growth cycle, high fecundity rates, transparency of embryogenesis via externally fertilized embryos, and the early generation of stereotyped visualizable behavior at embryonic stages [22–24]. In addition, zebrafish have been utilized as a model system for studying AD including studies examining tau-induced neurodegeneration [25], neuron-glia interactions in adult fish [26] and could serve as an excellent model to facilitate potential drug discovery in AD [27].

The goal of the present study was not to employ zebrafish as a model of AD *per se*, but to test whether a risk factor associated with AD could lead to toxicity or other potential negative consequences in an *in vivo* model. In this manner, the use of wild-type zebrafish embryos was used to extend our previous *in vitro* findings in transformed cells [16–18]. Our results demonstrate that exogenous treatment of zebrafish embryos with nApoE4_{1–151} led to an increase in toxicity and other morphological abnormalities. In addition, there was a trend towards decreased motor activation in the nApoE4_{1–151} treated-embryos as well as enhanced PHF-1 immunoreactivity. The findings of this study suggest that the single amino acid polymorphism

from ApoE3 to ApoE4 includes a toxic gain-of-function providing a possible link between harboring the *APOE4* gene and enhance risk associated with AD.

Materials and methods

Synthesis of nApoE₁₋₁₅₁ fragments

Generation of nApoE₄₁₋₁₅₁ and nApoE₃₁₋₁₅₁ including synthesis of plasmid, expression in *E. coli*, and purification (>85% purity) was contracted out to GenScript Inc. (Piscataway, NJ). An anti-6X His-tag at the C-terminal end was added to facilitate purification. The verification of proteins was confirmed by DNA sequencing, SDS PAGE, and Western blot by using standard protocols for molecular weight and purity measurements. The concentration of recombinant proteins was determined by Bradford protein assay with BSA as a standard. Characterization of nApoE₄₁₋₁₅₁ in our laboratory was assessed by ELISA and Western blot analysis utilizing an anti-His antibody as previously described [12]. A similar fragment to apoE3 (nApoE₃₁₋₁₅₁) was utilized in order to directly compare the differences in toxicity between nApoE₄₁₋₁₅₁ and nApoE₃₁₋₁₅₁. Full-length, human ApoE4 protein was purchased from Prosci Inc. (Poway, CA).

Zebrafish embryo care and maintenance

Animal husbandry and colony maintenance was handled by the Boise State University vivarium system. All animal protocols were coordinated with the Boise State University IACUC committee in accordance with recommendations from the Zebrafish Information Network (Zfin), IACUC protocol #AC18-011 and #AC21-009. Embryos were reared at 28.5°C in an enclosed incubation unit until treatment with exogenous protein fragments. Embryos were obtained for experiments by naturally breeding adult zebrafish in breeding tanks following Boise State University established standard operating procedures. The embryos were separated from adults and cleaned prior to the start of the experiment. All embryos were cultured in a temperature-controlled incubator for the duration of embryonic use. Juvenile zebrafish and embryos were under the care of BSU animal care staff unless used for experimentation. Sacrifices of treatment subjects were made following guidance of humane endpoints. Male and female *Danio rerio* (zebrafish) were used and their approximate average weight was approximately 1.5 g each. For the tail flick assays, we justified the number of animals that were used by the following calculation (power analysis software can be found at <http://www.cs.uiowa.edu/~rlenth/Power/>):

For the tail-flick test (TFT): Test selection: ANOVA for number of Tail Flicks per collection time point: Embryonic Testing (0-72hpf): WT: 3 Treatment Groups, N = 150 (total embryonic samples) n = 50 (samples per treatment), SD[treatment] = 0.1568, SD[within] = 0.5, Power = 0.8. A similar calculation was used and obtained for the TEMR behavioral assay. Pain and discomfort were assessed by experiment and appropriate anesthesia (tricaine) was applied to offset and reduce pain to animals.

Treatment of embryos with exogenous nApoE₁₋₁₅₁ fragments

Treatment of embryos began at 24 hpf during the 19-somite-prim-6 stage in accordance with the Kimmel Staging Series [24]. Zebrafish embryos that were staged at the time of treatment to be above 25 hours (prim-6) or below 19 hpf (20-somite stage) were excluded from experimentation. Incubation of embryos was accomplished using a mixture of E3 media (Cold Spring Harbor Protocols, recipe for E3 medium for zebrafish embryos; doi:10.1101/pdb.rec066449) with various concentrations of nApoE₄₁₋₁₅₁ or nApoE₃₁₋₁₅₁ protein fragments. Following staging assessments, embryos were allocated to an incubation chamber in an even distribution

depending on experiment. Embryos were kept with a density of no more than 5 embryos in a minimum of 100 μ l of E3 media + protein fragment per well in 96 well plates. Control groups were raised in identical conditions with the only difference being the absence of nApoE₁₋₁₅₁ fragments present in E3 media. Embryos were then placed in an incubator for 24 hours of undisturbed incubation at 28.5°C before being collected for experimentation.

Live imaging (Light Microscope)

Live observations were recorded on an EVOS M5000 Light Microscope using brightfield settings. Embryos were imaged at 4X for a general view of the embryo(s) and 10X or greater were used for tissue specific image acquisition. Mortality was assessed as described above by comparing the number of nominal labels (1 = Alive, 0 = Dead/Non-viable) given to each group. A tally was taken via a contingency table in R to provide a raw count for each individual treatment group. Normality and equal variance were tested for prior to analysis. Each group count was then tested against each other via a Chi-square analysis and displayed via a mosaic display to indicate statistical significance by shading and examination of the Pearson residual values.

Morphological assessments

A standardized scale was generated across multiple standards resulting in a developmental abnormality score (Fig 1). Embryos were scanned throughout the z-axis to identify internal flaws, verify pigmentation changes, and gauge organogenesis at specific stages in coordination with the Kimmel staging series as well as comparison to the non-treated controls.

Heart rate determination

Live imaging was also applied for mortality assessments of embryos in the manner of identifying heart rate over the course of 10 second intervals. If no heart rate was detected, stimulation of embryo through water movement was performed to verify lack of response to stimuli. If no response to stimulation was found in combination with a lack of heartbeat, the embryo was deemed non-viable. Heart rate was measured in a continuous manner by beats per minute (bpm) as described above. Samples were averaged by replicate to stabilize variation within groups. Five sets of heart rate collection dates were tested through two-way ANOVA modeling with three treatment groups (Control, nApoE₃₁₋₁₅₁, and nApoE₄₁₋₁₅₁) in R statistical software. ANOVA model was assessed for assumptions after creation of model in

Behavioral assays

Tail flick behavioral test. Larvae at 72 hpf were acclimated to the testing area for 2 minutes prior to experimentation. Five-minute videos were taken of each larvae using a Motic MGT 101 Moticam recording device with an LED-60T-B light ring. Videos were recorded down each treatment group column, then across well rows in a 96-well petri dish. Immediately following testing, the samples were euthanized using IACUC and University Guidelines, preserved in 4% PFA/PBT, then stored in 100% ethanol at -20°C. During each recording, individual larva was documented using a numerical code to designate treatment groups for a single-blind procedure, in which one researcher recorded and encoded video names for treatment and a second researcher analyzed coded videos. Scoring was completed by examining videos while documenting the number of spontaneous tail flicks in total for each larva over a 5-minute span. A single, spontaneous tail flick was determined by counting the number of times each larva bent their tail away from center and returned to the center axis. Samples were prepared by averaging 5 tail flicks per replicate over the course of 5 replicates with both nApoE₃₁₋₁₅₁ and

Scale for Developmental Abnormalities

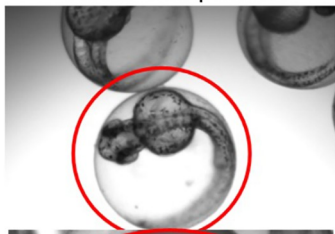
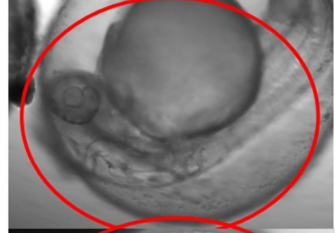
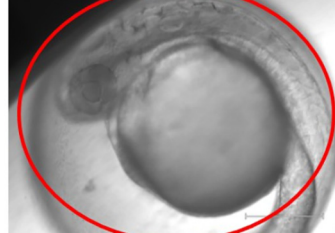


Descriptor	Characteristics	Score	Visual Comparison
No noticeable abnormalities	<ul style="list-style-type: none"> •Appears to match developmental markers •No abnormality can be visually identified •Proper pigmentation displayed 	0	
Minimal abnormality	<ul style="list-style-type: none"> •Does not meet one developmental standard •No observable hindbrain folding •Delay or lack of ear development •Deformed yolk sac •Enlarged cardiac cavity •Normal Pigmentation 	1	
Some abnormalities	<ul style="list-style-type: none"> •Does not meet two developmental standards •No observable hindbrain folding •Delay or lack of ear development •Deformed yolk sac •Enlarged cardiac cavity •Craniofacial abnormality 	2	
Severe abnormalities	<ul style="list-style-type: none"> •Does not meet three developmental standards •No observable hindbrain folding •Delay or lack of ear development •Deformed yolk sac •Enlarged cardiac cavity •Craniofacial abnormality 	3	
Extreme abnormality	<ul style="list-style-type: none"> •Meets any of the following standards: -No heart rate -No discernible shape -Blackened or cloudy 	4	

Fig 1. Semi-quantitative scale developed to assess morphological changes following treatment of zebrafish embryos with an amino-terminal fragment of nApoE4₁₋₁₅₁. Rubric for developmental abnormalities was accomplished in 48 hpf zebrafish following 24-hour treatment with 25 µg/ml of nApoE4₁₋₁₅₁. This scale was established to quantify the effects of nApoE4₁₋₁₅₁ as compared to untreated, control embryos. Identified hallmark defects that appeared consistently following treatment with nApoE4₁₋₁₅₁ included inflation of pericardial cavity, enlarged hearts, pigmentation alterations, and delays or lack of development in ear and brain structures. Data are representative of 10 embryos treated with 25 µg/ml nApoE4₁₋₁₅₁ per trial for a total of 30 embryos.

<https://doi.org/10.1371/journal.pone.0271707.g001>

nApoE4₁₋₁₅₁ at a final concentration of 25 µg/ml. Data analyzed for each trial represent the averaged results for each collection date. Data was analyzed through two-way ANOVA modeling with three treatment groups (Control, nApoE3₁₋₁₅₁, and nApoE4₁₋₁₅₁) in R statistical software. The ANOVA model was assessed for assumptions after creation of model in R.

Touch Evoked Movement Response Assay (TEMR)

Individual larvae at 72 hpf were moved to a 14x14 mm round glass bottom petri dish filled with E3 Media 2 minutes prior to testing for acclimation under light conditions for testing. Two-minute videos were recorded on Motic MGT 101 Moticam recording device with an LED-60T-B light ring. After the start of the recording at time (T = 0), embryos were tapped lightly with a blunt probe every 15 seconds. Directly following testing, larvae were euthanized using IACUC and University Guidelines, preserved in 4% PFA/PBT, then stored in 100% ethanol at -20°C. Videos were analyzed in Noldus Behavioral Software version 15.0. Criteria for scoring was based on the number of responses following the evoked stimulus. Data was grouped by treatment and analyzed in R statistical software. Data was assessed for normality and variance. The number of responses to the evoked stimulus was analyzed using One-Way ANOVA (aov; car package). A non-parametric Kruskal-Wallis test was applied to duration data as the data was not normal.

Immunofluorescence labeling

For all immunohistochemical procedures in this study, a standard protocol was followed for tissue preparation, and preparation of the slides. At the conclusion of treatment experiments, embryos were sacrificed prior to manual removal of chorion. Following de-chorionation, embryos were fixed in 4% paraformaldehyde (PFA)/phosphate buffered saline (PBS) overnight at 4°C and prepared for 5 µm paraffin-embedded sectioning using a Leica RM2235 Microtome at 4°C. Paraffin-embedded sections were used for staining following rehydration and a series of washes in PBS with tween-20 0.05% (PBST). Blocking of sections for non-specific staining was accomplished using a standard incubation buffer consisting of 1% normal goat serum, 2% bovine serum albumin in PBST for 2 hours at room temperature. Primary antibodies, detailed in Table 1, were incubated with slides for 18–24 hours at 4°C. Sections were then washed in triplicate for 5 minutes with PBST. Slides were then incubated in the appropriate secondary antibody for 1 hour at room temperature. Following the final wash, DAPI infused soft mount was placed on slides and allowed to set before coverslip addition. Sections were analyzed for preliminary staining with EVOS M5000 light cubes at lowest intensity settings. Sections were then kept in the dark at 4°C until used for confocal imaging. Following labeling, confocal assessment of the localization of nApoE4₁₋₁₅₁ in neuronal cell populations was as previously described [18]. All images and z-stacks generated were obtained using Zeiss Microscope, LSM 510 Meta confocal imaging system (Carl Zeiss, Oberkochen, Germany) and processed using Zen blue edition (Carl Zeiss, Göttingen, Germany). For each area of interest, a minimum of 3 sections per embryo were stained.

Results

We chose to examine the role of this specific amino-terminal fragment of nApoE4₁₋₁₅₁ for several reasons. First, we documented widespread evidence for this fragment in the human AD

Table 1. Description of antibodies used for immunofluorescence experiments.

Primary Antibodies	Source	Secondary Antibodies	Recognition
Anti-6X His Tag (1:500, Rabbit polyclonal)	Abcam, Inc.	AF 488 (1:500, Goat, Anti-Rabbit)	Reacts specifically with His-tagged ApoE3 or E4 fragments
NeuN (1:50, Mouse monoclonal)	Abcam, Inc. (1B7)	AF 555 (1:200, Donkey, Anti-Mouse)	Recombinant full-length NeuN
PHF-1 (1:250, Mouse polyclonal)	Dr. Peter Davies (Albert Einstein College of Medicine, Bronx, NY)	AF 555 1:200, Donkey, Anti-Mouse)	Serine-396 and serine-404 phosphorylated sites of tau

<https://doi.org/10.1371/journal.pone.0271707.t001>

brain, where it localized within nuclei of microglia and neurons [18]. Second, generation of this fragment was documented following incubation of full-length ApoE4 with matrix metalloproteinase-9 (MMP-9) [18]. Finally, recent data from our lab suggests that, *in vitro*, nApoE4₁₋₁₅₁ can traffic to the nucleus leading to toxicity and expression of inflammatory genes in BV2 microglia cells [16, 17, 28]. It is noteworthy that because zebrafish embryos do not yet express fully functional glial cells at 24 hpf including microglia [29], our study focused on the effects of nApoE4₁₋₁₅₁ on neuronal populations. We previously identified the nApoE4₁₋₁₅₁ fragment within neurons of the human AD brain [18]. The purpose of this current study is to expand those findings *in vivo*, by assessing the mechanisms by which this fragment may induce toxicity, developmental abnormalities, and behavior deficits in a model system consisting of zebrafish.

Morphological assessments

A semi-quantitative morphological assessment revealed treatment group specific phenotypes that were predominantly present in the nApoE4₁₋₁₅₁-treatment group. A scale was generated across multiple standards resulting in a developmental abnormality score (Fig 1).

Embryos were scanned throughout the z-axis to identify internal flaws, verify pigmentation changes, and gauge organogenesis at specific stages in coordination with the Kimmel staging series as well as comparison to the non-treated controls. Control groups were used to set a standard of comparison of which nApoE3₁₋₁₅₁ followed closely in most regards except for loss of pigmentation in both treated groups (blue arrows, Fig 2A–2C). Features most commonly observed for nApoE4₁₋₁₅₁ groups in addition to loss of pigmentation were lack of hindbrain folding at cerebellar primordium (orange arrows, Fig 2A–2C), as well as enlargement of the cardiac cavity (red arrow, Fig 2C). Quantification of morphological abnormalities are depicted in Fig 2D based on our standardized scale, with nApoE4₁₋₁₅₁ showing the most severe degree of changes following treatment with a significant increase in developmental abnormality scores compared to untreated controls. Heart rate measurements reported a significant decrease in the average heart rate compared to untreated controls at both low (25 µg/ml) and high concentrations of nApoE4₁₋₁₅₁ (50 µg/ml) (Fig 2E).

Survivability and mortality assessments

Survivability curves indicated that treatment of zebrafish embryos at 24 hpf lead to significant mortality. There was a 90–100% reduction in viable embryos 48 hours after treatment began (Fig 3A). In addition, nApoE4₁₋₁₅₁ treated-embryos failed to recover after removal of treatment media. The survivability of embryos following treatment with 25 µg/ml of nApoE4₁₋₁₅₁ was reduced by 50% within 24 hours of treatment (yellow dotted line), whereas at 50 µg/ml, it was reduced by 50% by 12 hours (green dotted line, Fig 3A). As a control, we also tested the impact of nApoE3₁₋₁₅₁ on survival. In this case, identical concentrations of nApoE3₁₋₁₅₁ had little impact on embryo survival following treatment even at the highest concentration of 50 µg/ml (<15%) (blue dashed line, Fig 3A).

Mortality data reported a high nApoE4₁₋₁₅₁ associated mortality compared to both nApoE3₁₋₁₅₁ and non-treatment groups (p-value compared to non-treated controls was 1.17×10^{-13}) (Fig 3B). nApoE3₁₋₁₅₁ and controls revealed a nearly identical mortality rate with <10% drop in mortality for nApoE3₁₋₁₅₁ compared to untreated controls. These results suggest that changing a single amino acid (C>R) at position 112 is sufficient to induce significant toxicity when zebrafish embryos are treated exogenously with nApoE4₁₋₁₅₁. We also tested the ability of human, full-length ApoE4 to induce mortality using the highest concentration tested for nApoE4₁₋₁₅₁ (50 µg/ml). As shown in S1D Fig, full-length ApoE4 had minimal effect on

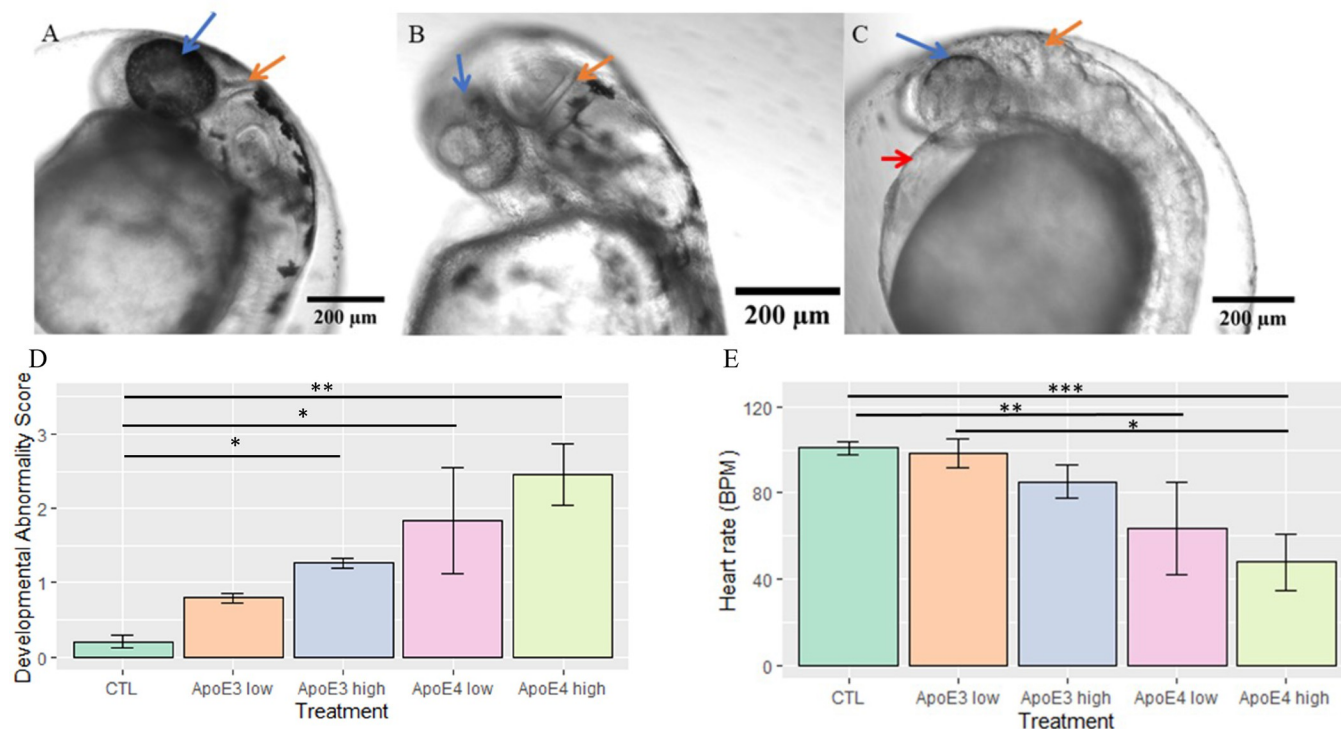


Fig 2. A sublethal concentration of nApoE4₁₋₁₅₁ leads to morphological abnormalities in zebrafish embryos at the hatching phase. Representative light phase contrast microscopic images following live imaging of embryos at 48 hpf following a 24-hour period with respective treatments (Control, 25 μg/ml of nApoE3₁₋₁₅₁, or 25 μg/ml of nApoE4₁₋₁₅₁). **A:** Arrows point to consistent morphological changes as compared to untreated controls that are healthy and categorized as having a developmental abnormality score of <1.0 (Panel A). The blue arrows designate pigmentation changes; orange arrows designate cerebellar primordium junction differences in the hindbrain. **B:** Exogenous treatment with nApoE3₁₋₁₅₁ impacted pigmentation pattern in otherwise healthy embryos. Embryos in this category were most likely to receive a score of <1. **C:** 24-hour incubation of a sublethal concentration of nApoE4₁₋₁₅₁ resulted in developmental abnormality scores >3. Embryos in this category were typically observed to be delayed in development with limited hindbrain folding (orange arrow), limited or lacking pigmentation (blue arrow), as well as enlargement of the cardiac cavity (red arrow). **D:** Quantitative developmental abnormality scores for each treatment group following treatment of embryos for 24 hours with respective fragments at low E3 (orange bar), E4 (pink bar) concentrations (25 μg/ml) or at high concentrations (50 μg/ml) E3 (gray bar), E4 (yellow bar). The nApoE4₁₋₁₅₁ 25 μg/ml-treated groups were significantly different from controls ($H(4) = -2.43, p = 0.0074$). At 50 μg/ml both nApoE4₁₋₁₅₁ ($H(4) = -3.32, p = 0.0004$) and nApoE3₁₋₁₅₁-treatment groups ($H(4) = -1.77, p = 0.037$) were significantly different from controls. Errors bars represent \pm S.E.M. * $p < 0.05$, ** $p < 0.01$, *** $p < 0.001$. **E:** Heart rate data obtained from live microscope analyses in 25 μg/ml and 50 μg/ml treatment groups nApoE3₁₋₁₅₁ and nApoE4₁₋₁₅₁ compared to non-treated controls. nApoE4₁₋₁₅₁ (pink bar, 25 μg/ml) was significantly different from controls ($H(4) = 1.77, p = 0.038$). nApoE4₁₋₁₅₁ (yellow bar, 50 μg/ml) was significantly different from nApoE3₁₋₁₅₁ 25 μg/ml ($H(4) = 1.94, p = 0.026$) and controls ($H(4) = 2.665, p = 0.0036$). Errors bars represent \pm S.E.M. All other comparisons were insignificant. * $p < 0.05$, ** $p < 0.01$, *** $p < 0.001$.

<https://doi.org/10.1371/journal.pone.0271707.g002>

toxicity and data were not significant different from non-treated controls. In contrast, treatment with nApoE4₁₋₁₅₁ lead to significant mortality (>90%, [S1D Fig](#)) as well as severe morphological damage ([S1A–S1C Fig](#)). Interesting, in non-treated controls all fish were healthy and alive but remained in their chorion (15/15 embryos, [S1A Fig](#)). For full-length ApoE4, 13/15 embryos were out of their chorion (87%) in three independent experiments. This data suggest that not only is full-length ApoE4 non-toxic, but that it actually accelerates hatching of zebrafish larvae.

Nuclear localization of nApoE4₁₋₁₅₁ and the presence of tau pathology

To assess the subcellular localization of nApoE4₁₋₁₅₁ following treatment of zebrafish embryos, confocal analysis was undertaken following fixation and sectioning of treated embryos. To track potential nApoE4₁₋₁₅₁ uptake, we utilized an anti-6X His-tag antibody (1:500), together with DAPI (nuclear stain) and markers for neuronal cells including Neuronal Nuclei (NeuN).

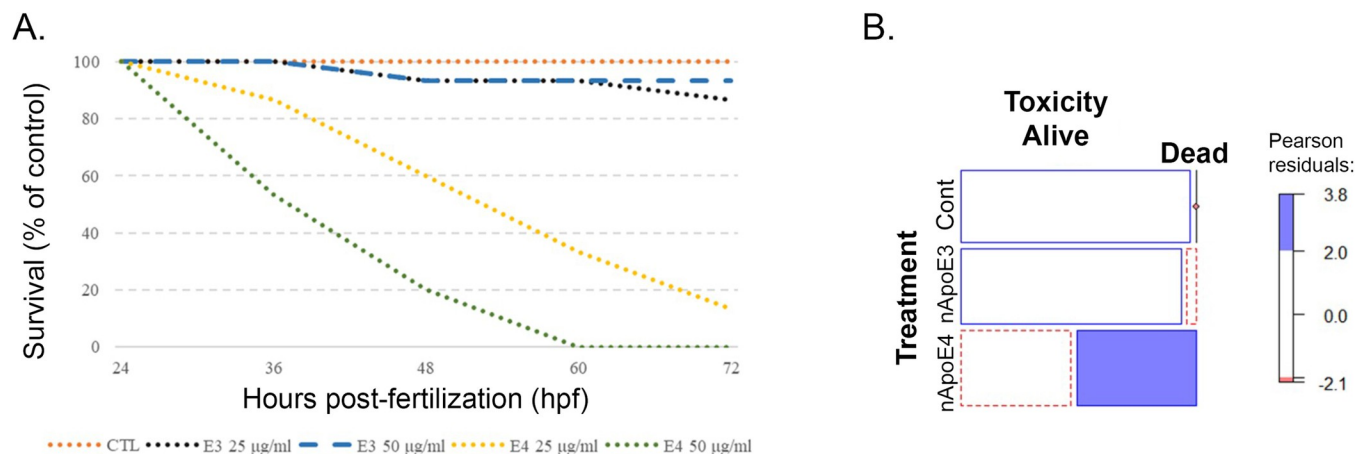


Fig 3. Survivability is decreased in zebrafish embryos following exogenous treatment with an amino-terminal fragment of nApoE4₁₋₁₅₁. A. Embryos at 24 hpf (prim-9 stage) were segregated into three groups: controls (untreated), 25 µg/ml or 50 µg/ml nApoE3₁₋₁₅₁, and 25 µg/ml or 50 µg/ml nApoE4₁₋₁₅₁. Embryos that lacked a heartbeat for 10 seconds were stimulated to induce movement. If no movement or heartbeat was detected, embryos were considered to be non-viable. Significant mortality was observed at both concentrations of nApoE4₁₋₁₅₁ by 48 hpf (orange and green dotted lines) compared to non-treated controls (orange dotted line) or nApoE3₁₋₁₅₁ (blue dashed line and black dotted lines). $N = 3$ independent trials, $N = 5$ fish/treatment. B. The Mosaic Plot depicts mortality based on a lack of heartbeat and response to physical stimuli following exogenous treatment of 48 hpf zebrafish embryos with either 25 µg/ml nApoE3₁₋₁₅₁ or nApoE4₁₋₁₅₁ for 24 hours. The blue filled region of the bar graph designates 25 µg/ml treatment of nApoE4₁₋₁₅₁ which led to a significant portion of the embryos being designated as dead. The red dotted portion of the bar graphs indicates less than expected were alive ($p = 1.17 \times 10^{-13}$). All blank cells indicate the sample group followed the estimated trend. Data indicated significant mortality for only the nApoE4₁₋₁₅₁ group. $N = 3$ independent experiments, 15 embryos/treatment.

<https://doi.org/10.1371/journal.pone.0271707.g003>

NeuN is part of the RNA splicing machinery and is predominantly found in the nucleus of post-mitotic neurons [30]. As depicted in Fig 4B, nApoE4₁₋₁₅₁ is taken up by neurons following exogenous treatment of 48 hpf zebrafish embryos that colocalized with NeuN (Fig 4B and 4C). Of interest was the punctate staining of nApoE4₁₋₁₅₁ which supports our previous staining pattern observed in transformed BV2 microglial cells, suggesting possible aggregation of the nApoE4₁₋₁₅₁ fragment [18]. Also displayed in Fig 4 is staining from a representative, whole embryo mount taken at 10X magnification. Staining of nApoE4₁₋₁₅₁ is noted throughout the nervous system (green labeling, Fig 4D). Strong co-localization between nApoE4₁₋₁₅₁ and NeuN was noted in the region of the medulla (arrows, Fig 4D).

Additional immunofluorescence studies were undertaken to assess any potential relevance to known AD pathology. Previous studies have demonstrated that amino-terminal fragments of ApoE4 localize in NFTs of the human AD brain [12] and may induce neurofibrillary changes in cultured neurons [11]. Zebrafish are known to express gen orthologues to the human *MAPT* gene including *MAPTA* and *MAPTB* [31]. Therefore, we examined whether treatment of zebrafish embryos with nApoE4₁₋₁₅₁ led to similar pathological changes to tau by confocal IF using PHF-1 that recognizes hyperphosphorylated, fibrillar forms of tau present in the human AD brain. For these experiments we used embryos at 72 hpf due to our preliminary findings that staining of PHF-1 in 48 hpf was relatively weak following treatment. Robust labeling of PHF-1 within apparent neurons was evident under these experimental conditions (arrows, Fig 5I–5L). In contrast, little PHF-1 labeling was observed with nApoE3₁₋₁₅₁ under identical experimental conditions (Fig 5E–5H). In Fig 5K, a merged, high-magnification of another representative treated embryo is shown. In this case, PHF-1 labeling appeared fibrillar in nature, which is characteristic of PHF-1 staining within NFTs of the AD brain [32]. These results support the linkage of nApoE4₁₋₁₅₁ to one of the significant hallmark pathologies found in AD, namely neurofibrillary tangles.

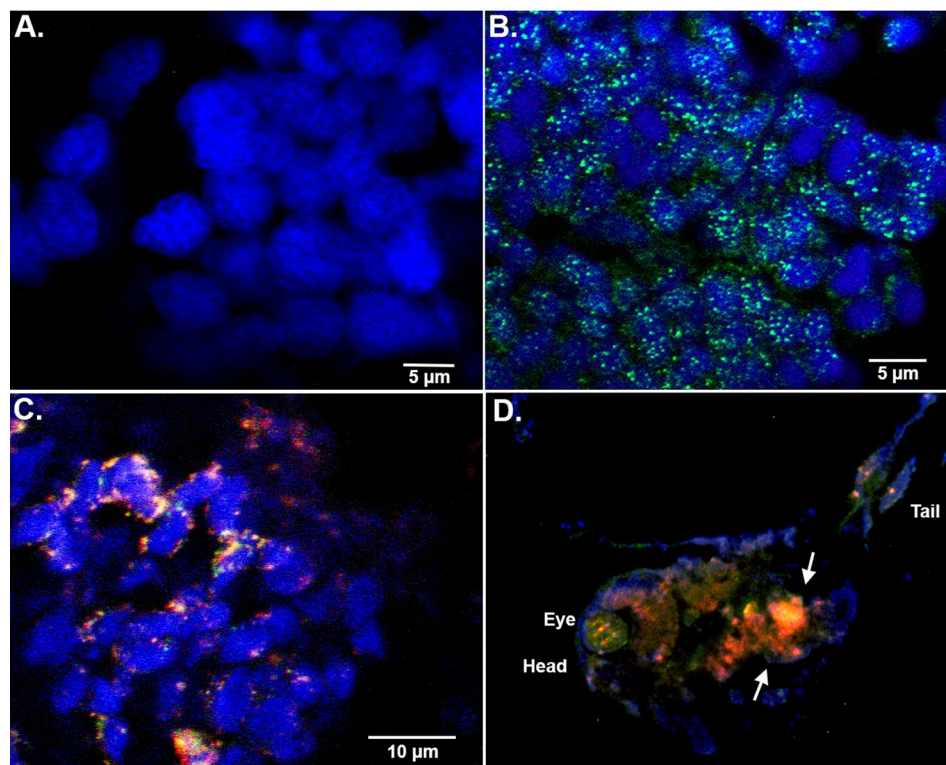


Fig 4. Exogenous treatment of zebrafish embryos with nApoE4₁₋₁₅₁ leads to nuclear localization. A-C. Representative images from confocal immunofluorescence in 5 mm paraffin-embedded sections that were stained with DAPI (A), anti-His antibody (green, B), or anti-His together with NeuN (C). There was no detection of nApoE4₁₋₁₅₁ fragments in untreated control neuronal cells as indicated by the lack of labeling in Panel A. Nuclear localization of the nApoE4 fragment was evident (Panels B and C) following exogenous treatment. For the E4 fragment, staining appears punctate and co-localized with NeuN and DAPI (B and C). All images were captured within the area of the cerebellum and fourth ventricle. **D.** Identical to Panels B-C with the exception that whole embryo mounts were triple labeled in order to display overall labeling in the entire organism at low magnification. Labeling of head, eye and tail is presented for orientation. The intense orange fluorescence area (arrows) represents regions with strong overlap between the E4 fragment and NeuN. In this case, labeling of the E4 fragment that co-localized with DAPI and NeuN was apparent in the hindbrain brain region. Data are representative of five independent experiments.

<https://doi.org/10.1371/journal.pone.0271707.g004>

Motor deficits in juvenile zebrafish following treatment with a sublethal concentration of nApoE4151

As an initial approach, we assessed whether a stereotypical motor behavior in zebrafish, spontaneous tail flicking, was diminished following treatment with nApoE4₁₋₁₅₁ or nApoE3₁₋₁₅₁. For these experiments only fish that were deemed viable and without noticeable, severe morphological abnormalities were utilized. Fig 6A depicts the results of this experiment showing that zebrafish treated with nApoE4₁₋₁₅₁ performed the least number of tail flicks per group with >50% reduction from untreated controls. Treatment of zebrafish larvae with nApoE3₁₋₁₅₁ performed similarly to controls. However, no difference was significant across any group ($F(2,27) = 1.24, p = 0.305$). It's noteworthy that control zebrafish demonstrated minimal spontaneous tail flick behavior and there were large variations within groups. The lack of response in even our control cohorts indicates that there is limited motor movement in 72 hpf in an unstimulated environment. Therefore, a second motor behavior task was undertaken whereby zebrafish were stimulated to move using a blunt instrument. This type of behavior is known as the touch-evoked movement response (TEMR) test and results mirrored the findings from the spontaneous tail-flick experiment (Fig 6B). In this case, control and nApoE3151-treated

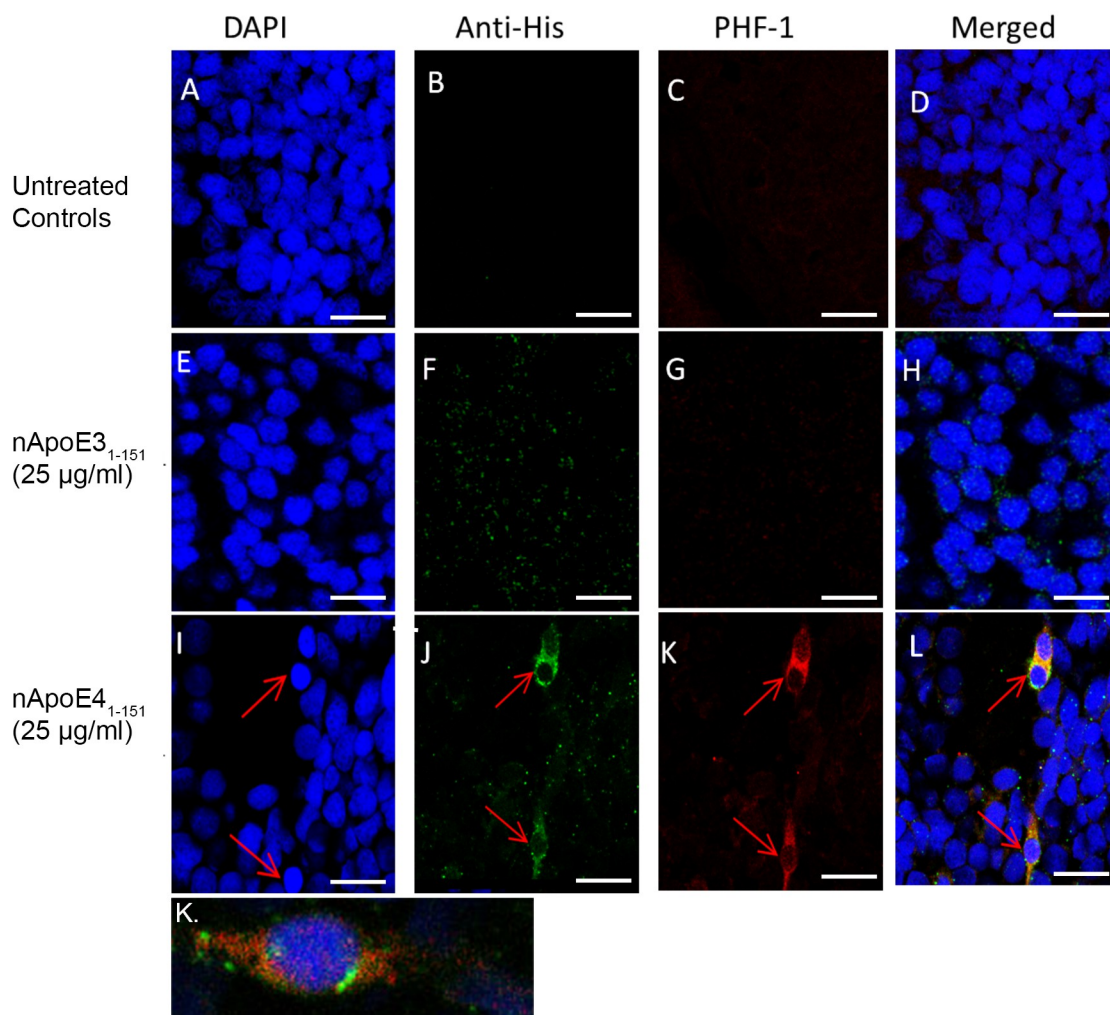


Fig 5. Tau pathology present after treatment with exogenous nApoE4₁₋₁₅₁ fragment in 72 hpf zebrafish brain. Representative 40X images from confocal immunofluorescence in 5 mm paraffin embedded sections of non-treated control 72 hpf zebrafish (A-D), nApoE3₁₋₁₅₁-treated at 25 μg/ml (E-H), or nApoE4₁₋₁₅₁-treated at 25 μg/ml (I-L). Strong PHF-1 labeling was only observed following treatment with nApoE4₁₋₁₅₁ (I-L). Panel K depicts a separate, representative merged image following treatment with nApoE4₁₋₁₅₁. In this case, at high magnification the fibrillar nature of PHF-1 labeling was apparent. All scale bars represent 50 μm. Data are representative of three independent experiments.

<https://doi.org/10.1371/journal.pone.0271707.g005>

groups responded to 90% of applied stimulations. In contrast, nApoE4₁₅₁-treated fish responded to fewer than 50% of evoked stimulations (Sup1-3 video files). However, as in Fig 6A, due to high variations within groups, no statistical significance was observed ($F(12) = 1.482$, $p = 0.266$). We also assessed the total distance traveled as well as the cumulative duration of response during the TEMR test and in this case both nApoE3 and E4 groups showed a downward trend although similar to the previous findings, no significant differences (p -value < 0.05) between groups were observed (Fig 6C and 6D). Taken together, our results show strong trends for motor behavior impairments following treatment of zebrafish with sub-toxic concentrations of nApoE4₁₅₁, that were not present in non-treated controls.

Due to the observations that tail flick behavior was abnormal following treatment of embryos with nApoE4₁₋₁₅₁, we examined PHF-1 and nApoE4₁₋₁₅₁ staining in the developing

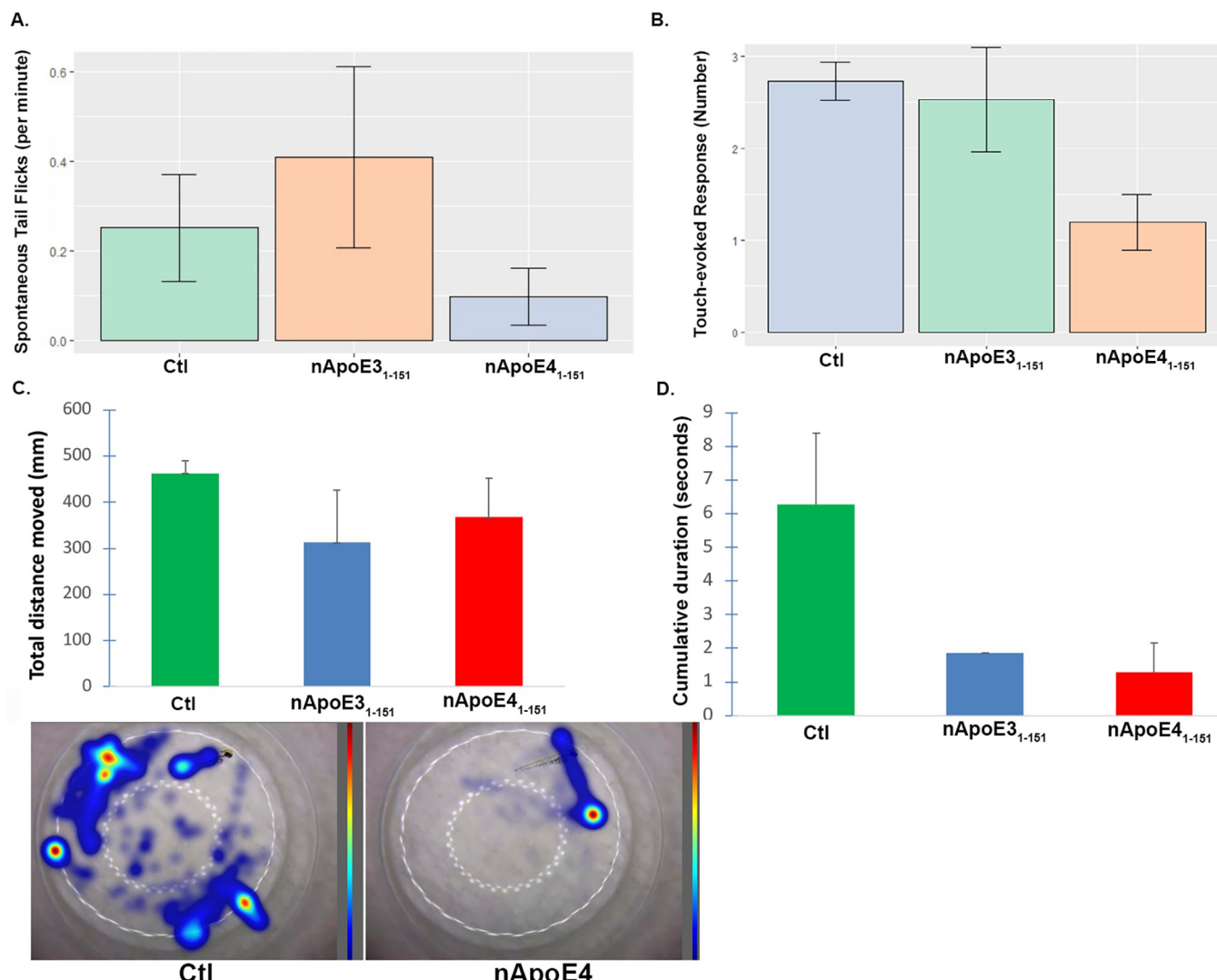


Fig 6. Negative trends in motor behavior in zebrafish following treatment with nApoE4₁₋₁₅₁. A. Groups for non-treated controls (green bar), nApoE3₁₋₁₅₁ 25 µg/ml (orange bar), and ApoE4₁₋₁₅₁ 25 µg/ml (blue bar) were assessed via video monitoring to determine number of spontaneous tail flicks per minute that were then averaged per group for each trial. Data are representative of N = 5 trials, for a total of 25 embryos per group, ±SEM. Data depicted show limited spontaneous tail flick activation from every group with no difference detectable between groups ($F(2,27) = 1.24, p = 0.305$). B. Results from the touch-evoked response motor behavior experiment. Non-treated controls had a 90% response rate to the evoked, tactile stimulus, whereas for nApoE4₁₋₁₅₁-treated groups responded to fewer than 50% of stimuli. No significant difference was observed ($F(12) = 1.482, p = 0.266$). C and D. Results from TEMR analyses similar to Panels A and B with the exception that in this case, total distance traveled (C) or the total time swimming (D) were recorded via video monitoring and using Noldus tracking software. For Panel C, representative heat maps of individual larvae representing either wild-type controls (left Panel), or a low-performing nApoE4₁₋₁₅₁-treated zebrafish (right Panel). Each bar represents the average total distance traveled or averaged cumulative duration during 5 independent trials, for a total of 15 embryos per group, (±SEM). No significant differences were observed, with for example the Ctl group vs. nApoE4₁₋₁₅₁ having a p value = 0.08 in Panel C. P-values for Panel D were Ctl vs. E3 fragment = 0.86 and Ctl vs. E4 fragment = 0.06.

<https://doi.org/10.1371/journal.pone.0271707.g006>

tail region by confocal microscopy. As shown in Fig 7, typical punctate nApoE4₁₋₁₅₁ labeling was observed in apparent skeletal muscle cells (Fig 7E). However, in this case, we were unable to identify nuclear localization of the fragment within muscle cell populations. Instead, it appeared most labeling was cytoplasmic (Fig 7F). In nApoE4₁₋₁₅₁-treated embryos we observed skeletal muscle formations that appeared disorganized with cells exhibiting abnormal morphologies (Fig 7E). These data could explain the motor behavioral deficits even following removal of treatment media.

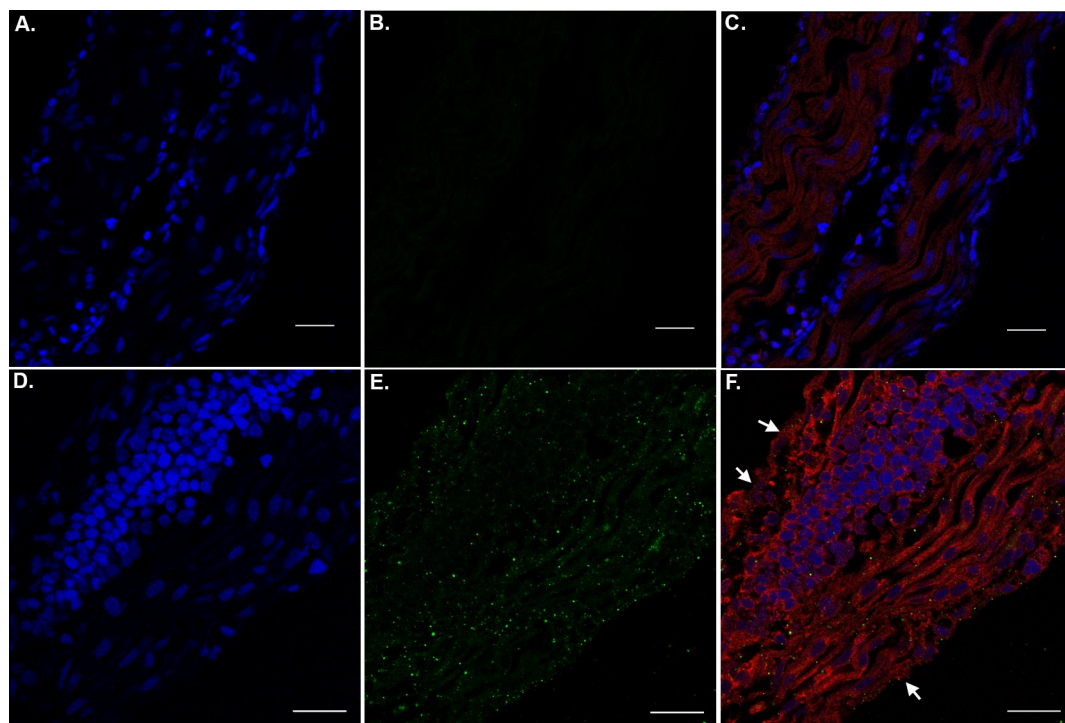


Fig 7. The presence of nApoE4₁₋₁₅₁ within tail regions of zebrafish embryos. A–C: Representative images from confocal immunofluorescence in 5 mm paraffin-embedded sections of non-treated control 48 hpf zebrafish embryos that were stained with DAPI (A), anti-His antibody (1:500) (B), and the merged image together with PHF-1 (1:250) in Panel (C). There was no detection of any nApoE4₁₋₁₅₁ fragments in untreated control sections as indicated by the lack of labeling in Panel B. D–F: Identical to Panels A–D with the exception that embryos were exogenously treated for 24 hours with 25 µg/ml of nApoE4₁₋₁₅₁. In this case punctate staining of the fragment was observed that appeared cytoplasmic. PHF-1 labeling was identified in muscle cells that exhibited abnormal morphology (arrows, Panel F). All scale bars represent 20 µm.

<https://doi.org/10.1371/journal.pone.0271707.g007>

Discussion

Despite intensive research efforts, the pathophysiological relationship between harboring the *APOE4* allele and the development of late-onset AD remains largely unknown. This question is further complicated by the fact that only the ApoE4 protein represents a significant risk factor even though it differs from ApoE3 by a single amino acid at position 112 and ApoE2 by two amino acids (positions 112 and 158) [6]. Both substitutions lead to the replacement of a cysteine residue with an arginine residue [6]. One possible hypothesis leading to increased dementia risk is the propensity of the ApoE4 isoform to be highly susceptible to proteolysis compared to E3 and E2 [33]. Prior research from our lab supports the hypothesis that ApoE4 fragmentation via the metalloproteinase-9 (MMP-9) may contribute to AD pathology and inflammation [18]. Additional studies have also shown neurotoxic and pro-inflammatory responses to the fragmentation of ApoE4 [34–37]. Recently we identified a 151 amino-terminal fragment of ApoE4 (nApoE4₁₋₁₅₁) that localized within the nucleus of both neurons and microglia cells of the human AD brain [18] and *in vitro*, we demonstrated this fragment is taken up by BV2 microglia cells, traffics to the nucleus and leads to the upregulation of thousands of genes, many of which associated with microglia activation and inflammation [16, 28].

In the current studies, we expanded these findings utilizing an *in vivo* model system consisting of zebrafish. The primary weakness in our previous published work was the use of transformed, BV2 microglia cells in an entirely *in vitro* model system. These weaknesses can be summarized as relying on data from a single, murine, immortal microglia cells that may not be

representative of normal, non-transformed cells. Another potential caveat of our previous studies was the reliance upon *in vitro* model systems to investigate the pathophysiological actions of nApoE4₁₋₁₅₁. Therefore, the primary goal of the current study was to expand our *in vitro* findings to an intact organism consisting of zebrafish embryos and larvae. Zebrafish have emerged as an excellent model organism for studies of vertebrate biology. One of the more distinct advantages of the zebrafish is the optical clarity of the embryos allowing for the investigation throughout the developmental process using non-invasive imaging techniques. There is also a high degree of conservation between zebrafish and human brain organization including both neuroanatomic [38, 39], neurochemical [40], and behavioral circuitry including learning [41], touch [42], and decision making [43]. Moreover, zebrafish have served as excellent models to study the pathophysiology underlying AD including a study that demonstrated intraventricular injection of A β ₁₋₄₂ in the embryonic brain leads to memory loss and cognitive deficits along with increased tau phosphorylation [44, 45]. Taken together, the zebrafish presents itself as a novel model system to examine the potential effects of nApoE4₁₋₁₅₁ and we choose to examine wild-type zebrafish only so that the potential effects of nApoE4₁₋₁₅₁ could be examined singularly without any potential confounding variables that could arise in mutant zebrafish harboring APP or tau mutations.

As an initial approach, we treated zebrafish embryos at 24 hpf and examined any potential morphological changes 24 hours later (48 hpf). Compared to untreated controls, nApoE4₁₋₁₅₁ exposure produced significant toxicity and led to changes to the nervous system, the heart, and loss of pigmentation. The nervous system was visibly impacted by the lack of hindbrain folding that is typical in 48 hpf zebrafish along the cerebellar primordium. Additionally, nApoE4₁₋₁₅₁ treatments at both a low (25 μ g/ml) and high (50 μ g/ml) concentrations produced significant differences from controls in terms of developmental abnormalities and reduced heart rates. The morphological results of enlargement of hearts following nApoE4₁₋₁₅₁ treatment are intriguing based on the well-known link between inheritance of APOE4 and an increased risk of cardiovascular disease [46]. Confocal imaging revealed the colocalization of nApoE4₁₋₁₅₁ with NeuN within the hindbrain region around the medulla oblongata which regulates heart rate. These data support the hypothesis that nApoE4₁₋₁₅₁ may destabilize the hindbrain networks during the incubation period leading to downstream cardiovascular deficits, including a reduced heart rate.

From early stages of development, zebrafish swimming behavior and response to external stimuli can be assessed. The responses to external stimuli can be detected at early larvae states (72 hpf) in which zebrafish show escape response swimming behavior, for example in response to touch directed to either the head or tail [47]. Similar to the cardiovascular system, the touch-evoked response is under control of the hindbrain [48, 49]. Specifically, the touch escape response and spontaneous tail flicks are both proposed to be regulated by the Mauthner cells located in the zebrafish hindbrain [50, 51]. Treatment of zebrafish larvae with nApoE4₁₋₁₅₁ led to less than half of the stimulation attempts whereas non-treated controls and nApoE3₁₋₁₅₁ responded to over 90% and 80% stimulation attempts, respectively. Downward trends for both total distances swam, and duration times were also observed following treatment with nApoE4₁₋₁₅₁, that just missed statistical significance. Increased detection of nApoE4₁₋₁₅₁ compared to controls within the hindbrain region could be the rationale for the effects observed in both of these locomotor assays. Presently, it is not known how nApoE4₁₋₁₅₁ leads to these motor deficits or at what stage of this behavior does nApoE4₁₋₁₅₁ interfere: initiation or execution of the behavioral response? Initiation of the response would imply the sensation of the stimulus was never received through the rohon-beard cells or the dorsal root ganglia which have been shown to share the responsibility of tactile sensation during the 72 hpf period [52].

Another finding in the present study was enhanced mortality induced by exogenous treatment of nApoE4₁₋₁₅₁, which was not observed in parallel experiments with nApoE3₁₋₁₅₁ nor following treatment with full-length, human ApoE4. These results support our previous *in vitro* findings indicating enhanced cellular toxicity of only nApoE4₁₋₁₅₁, which differs by a single amino acid at position 112 (R>C) [18]. The further identification of nApoE4₁₋₁₅₁, within the nucleus of neurons of the developing nervous system of zebrafish supports the hypothesis that the uptake of this fragment and trafficking to the nucleus may lead to stimulation of cell death pathways similar to what we have recently observed in BV2 microglia cells [16, 28].

In the context of AD, an important finding of our results was the evolution of tau pathology following exogenous treatment of zebrafish with nApoE4₁₋₁₅₁ at 72 hpf. These findings support that nApoE4₁₋₁₅₁ may promote tau pathology, a hallmark feature seen in human AD pathology [53]. Previous studies have linked the presence of amino-terminal fragments of ApoE4 with NFTs in the human AD brain as well as in various animal models including following expression of mutant forms of tau in zebrafish [15, 25, 33]. The observed tau pathology can lead to disruptions in axonal function which in turn, can have deleterious effects on neuronal signaling and axonal transport [54, 55].

A final observation was staining within skeletal muscle located within the tail region of developing zebrafish (Fig 7). We observed skeletal muscle formations that appeared disorganized with cells exhibiting abnormal morphologies. These data could explain the motor behavioral deficits even following removal of treatment media. Our results are similar in terms of muscle cell disorganization observed in zebrafish expressing mutant acetylcholine receptors at the neuromuscular junction [56]. Further experiments will be necessary to fully understand how nApoE4₁₋₁₅₁ may be exerting this effect in skeletal muscle.

Conclusion

The *APOE4* allele stands out as the greatest risk factor for late-onset AD, as *APOE4* carriers account for 65–80% of all cases [57]. Although ApoE4 plays a normal role in lipoprotein transport, how it contributes to AD pathogenesis remains speculative. Recent data from our lab suggests that, *in vitro*, nApoE4₁₋₁₅₁ can traffic to the nucleus leading to toxicity and expression of inflammatory genes in BV2 microglia cells [16, 18, 28]. In the present study, we now expand those findings *in vivo*, by demonstrating toxicity of nApoE4₁₋₁₅₁, and motor behavior deficits in a novel model system consisting of zebrafish. Taken together, these results support the hypothesis that a key step in mechanism of action is the cleavage of full-length ApoE4, generating an amino-terminal fragment that exhibits a toxic-gain of function. Therefore, the neutralization of this amino-terminal fragment of ApoE4, specifically, may serve as an important therapeutic strategy in the treatment of AD.

Supporting information

S1 Fig. Full-length ApoE4 does not induce toxicity in zebrafish embryos. Representative images displaying morphological effects following treatment with either 50 µg/ml full-length ApoE4 (B) or nApoE4₁₋₁₅₁ (C) indicated that full-length ApoE4 showed little effects on morphology as compared to non-treated controls (A). Embryos treated with full-length ApoE4 resulted in 13/15 fish had exiting their chorion. In contrast, significant morphological effects (arrow, C) and mortality were observed in the nApoE4₁₋₁₅₁-treatment group (D). Data are representative of three independent experiments (N = 5 per group). No significant difference was observed in mortality between non-treated controls and full-length ApoE4 (p = 0.19). Significant mortality (93%) was observed in the nApoE4₁₋₁₅₁-treatment group (p = .000076). (TIF)

S1 Video. Raw video file depicting a representative wild-type zebrafish recorded during the TEMR behavior test. Two-minute videos were recorded on Motic MGT 101 Moticam recording device with an LED-60T-B light ring. After the start of the recording at time (T = 0), embryos were tapped lightly with a blunt probe every 15 seconds. See details in materials and methods section.

(MP4)

S2 Video. Representative raw video file depicting a representative nApoE4₁₋₁₅₁-treated zebrafish recorded during the TEMR behavior test. Two-minute videos were recorded on Motic MGT 101 Moticam recording device with an LED-60T-B light ring. After the start of the recording at time (T = 0), embryos were tapped lightly with a blunt probe every 15 seconds. See details in materials and methods section.

(MP4)

S3 Video. Representative raw video file depicting a representative nApoE4₁₋₁₅₁-treated zebrafish recorded during the TEMR behavior test. Two-minute videos were recorded on Motic MGT 101 Moticam recording device with an LED-60T-B light ring. After the start of the recording at time (T = 0), embryos were tapped lightly with a blunt probe every 15 seconds. See details in materials and methods section.

(MP4)

Author Contributions

Conceptualization: Madyson M. McCarthy, Saylor E. Leising, Amelia S. Cogan, Jonathon C. Reeck, Julia T. Oxford, Troy T. Rohn.

Data curation: Madyson M. McCarthy, Makenna J. Hardy, Saylor E. Leising, Erica S. Stewart, Amelia S. Cogan, Troy T. Rohn.

Formal analysis: Madyson M. McCarthy, Makenna J. Hardy, Saylor E. Leising, Erica S. Stewart, Amelia S. Cogan, Katie Matteo, Jonathon C. Reeck.

Funding acquisition: Julia T. Oxford, Troy T. Rohn.

Investigation: Makenna J. Hardy, Saylor E. Leising, Alex M. LaFollette, Erica S. Stewart, Amelia S. Cogan, Tanya Sanghal, Katie Matteo.

Methodology: Madyson M. McCarthy, Jonathon C. Reeck.

Project administration: Julia T. Oxford, Troy T. Rohn.

Resources: Julia T. Oxford, Troy T. Rohn.

Supervision: Jonathon C. Reeck, Julia T. Oxford, Troy T. Rohn.

Validation: Makenna J. Hardy.

Visualization: Makenna J. Hardy, Saylor E. Leising.

Writing – original draft: Madyson M. McCarthy, Makenna J. Hardy, Troy T. Rohn.

Writing – review & editing: Troy T. Rohn.

References

1. DeTure MA, Dickson DW. The neuropathological diagnosis of Alzheimer's disease. *Molecular neurodegeneration*. 2019; 14(1):32. Epub 2019/08/04. <https://doi.org/10.1186/s13024-019-0333-5> PMID: 31375134; PubMed Central PMCID: PMC6679484.

2. Martins IJ, Hone E, Foster JK, Sunram-Lea SI, Gnjec A, Fuller SJ, et al. Apolipoprotein E, cholesterol metabolism, diabetes, and the convergence of risk factors for Alzheimer's disease and cardiovascular disease. *Molecular psychiatry*. 2006; 11(8):721–36. Epub 2006/06/21. <https://doi.org/10.1038/sj.mp.4001854> PMID: 16786033.
3. As Association. Alzheimer's Association Report 2018 Alzheimer's disease facts and figures. *Alzheimer's & Dementia*. 2018; 14:367–429.
4. Pradhan LK, Sahoo PK, Chauhan S, Das SK. Recent Advances Towards Diagnosis and Therapeutic Fingerprinting for Alzheimer's Disease. *J Mol Neurosci*. 2022; 72(6):1143–65. Epub 2022/05/14. <https://doi.org/10.1007/s12031-022-02009-7> PMID: 35553375.
5. Munoz SS, Li H, Ruberu K, Chu Q, Saghatelian A, Ooi L, et al. The serine protease HtrA1 contributes to the formation of an extracellular 25-kDa apolipoprotein E fragment that stimulates neuritogenesis. *J Biol Chem*. 2018; 293(11):4071–84. Epub 2018/02/08. <https://doi.org/10.1074/jbc.RA117.001278> PMID: 29414786; PubMed Central PMCID: PMC5857987.
6. Weisgraber KH. Apolipoprotein E: structure-function relationships. *Adv Protein Chem*. 1994; 45:249–302. Epub 1994/01/01. [https://doi.org/10.1016/s0065-3233\(08\)60642-7](https://doi.org/10.1016/s0065-3233(08)60642-7) PMID: 8154371.
7. Innerarity TL, Mahley RW. Enhanced binding by cultured human fibroblasts of apo-E-containing lipoproteins as compared with low density lipoproteins. *Biochemistry*. 1978; 17(8):1440–7. Epub 1978/04/18. <https://doi.org/10.1021/bi00601a013> PMID: 206278
8. Goldstein JL, Brown MS. The LDL pathway in human fibroblasts: a receptor-mediated mechanism for the regulation of cholesterol metabolism. *Curr Top Cell Regul*. 1976; 11:147–81. Epub 1976/01/01. <https://doi.org/10.1016/b978-0-12-152811-9.50011-0> PMID: 187385
9. Xie C, Lund EG, Turley SD, Russell DW, Dietschy JM. Quantitation of two pathways for cholesterol excretion from the brain in normal mice and mice with neurodegeneration. *Journal of lipid research*. 2003; 44(9):1780–9. Epub 2003/06/18. <https://doi.org/10.1194/jlr.M300164-JLR200> PMID: 12810827.
10. Buttini M, Orth M, Bellosta S, Akeefe H, Pitas RE, Wyss-Coray T, et al. Expression of human apolipoprotein E3 or E4 in the brains of ApoE^{-/-} mice: isoform-specific effects on neurodegeneration. *J Neurosci*. 1999; 19(12):4867–80. Epub 1999/06/15. <https://doi.org/10.1523/JNEUROSCI.19-12-04867.1999> PMID: 10366621; PubMed Central PMCID: PMC6782676.
11. Harris FM, Brecht WJ, Xu Q, Tesseur I, Kekoni L, Wyss-Coray T, et al. Carboxyl-terminal-truncated apolipoprotein E4 causes Alzheimer's disease-like neurodegeneration and behavioral deficits in transgenic mice. *Proc Natl Acad Sci U S A*. 2003; 100(19):10966–71. <https://doi.org/10.1073/pnas.1434398100> PMID: 12939405.
12. Rohn TT, Catlin LW, Coonse KG, Habig JW. Identification of an amino-terminal fragment of apolipoprotein E4 that localizes to neurofibrillary tangles of the Alzheimer's disease brain. *Brain Res*. 2012; 1475:106–15. <https://doi.org/10.1016/j.brainres.2012.08.003> PMID: 22902767.
13. Harris FM, Brecht WJ, Xu Q, Mahley RW, Huang Y. Increased tau phosphorylation in apolipoprotein E4 transgenic mice is associated with activation of extracellular signal-regulated kinase: modulation by zinc. *J Biol Chem*. 2004; 279(43):44795–801. Epub 2004/08/24. <https://doi.org/10.1074/jbc.M408127200> PMID: 15322121.
14. Brecht WJ, Harris FM, Chang S, Tesseur I, Yu GQ, Xu Q, et al. Neuron-specific apolipoprotein e4 proteolysis is associated with increased tau phosphorylation in brains of transgenic mice. *J Neurosci*. 2004; 24(10):2527–34. <https://doi.org/10.1523/JNEUROSCI.4315-03.2004> PMID: 15014128.
15. Munoz SS, Garner B, Ooi L. Understanding the Role of ApoE Fragments in Alzheimer's Disease. *Neurochem Res*. 2019; 44(6):1297–305. Epub 2018/09/19. <https://doi.org/10.1007/s11064-018-2629-1> PMID: 30225748.
16. Pollock TB, Cholico GN, Isho NF, Day RJ, Suresh T, Stewart ES, et al. Transcriptome Analyses in BV2 Microglial Cells Following Treatment With Amino-Terminal Fragments of Apolipoprotein E. *Frontiers in aging neuroscience*. 2020; 12:256. Epub 2020/09/15. <https://doi.org/10.3389/fnagi.2020.00256> PMID: 32922284; PubMed Central PMCID: PMC7456952.
17. Pollock TB, Mack JM, Day RJ, Isho NF, Brown RJ, Oxford AE, et al. A Fragment of Apolipoprotein E4 Leads to the Downregulation of a CXorf56 Homologue, a Novel ER-Associated Protein, and Activation of BV2 Microglial Cells. *Oxid Med Cell Longev*. 2019; 2019:5123565. Epub 2019/06/15. <https://doi.org/10.1155/2019/5123565> PMID: 31198491; PubMed Central PMCID: PMC6526552.
18. Love JE, Day RJ, Gause JW, Brown RJ, Pu X, Theis DI, et al. Nuclear uptake of an amino-terminal fragment of apolipoprotein E4 promotes cell death and localizes within microglia of the Alzheimer's disease brain. *Int J Physiol Pathophysiol Pharmacol*. 2017; 9(2):40–57. Epub 2017/05/24. PMID: 28533891; PubMed Central PMCID: PMC5435672.
19. Matsui H, Ito J, Matsui N, Uechi T, Onodera O, Kakita A. Cytosolic dsDNA of mitochondrial origin induces cytotoxicity and neurodegeneration in cellular and zebrafish models of Parkinson's disease.

- Nat Commun. 2021; 12(1):3101. Epub 2021/05/27. <https://doi.org/10.1038/s41467-021-23452-x> PMID: 34035300; PubMed Central PMCID: PMC8149644.
20. Bashirzade AA, Zabegalov KN, Volgin AD, Belova AS, Demin KA, de Abreu MS, et al. Modeling neurodegenerative disorders in zebrafish. *Neurosci Biobehav Rev*. 2022; 138:104679. Epub 2022/05/02. <https://doi.org/10.1016/j.neubiorev.2022.104679> PMID: 35490912.
 21. Thawkar BS, Kaur G. Zebrafish as a Promising Tool for Modeling Neurotoxin-Induced Alzheimer's Disease. *Neurotox Res*. 2021; 39(3):949–65. Epub 2021/03/10. <https://doi.org/10.1007/s12640-021-00343-z> PMID: 33687726.
 22. Maharajan K, Muthulakshmi S, Nataraj B, Ramesh M, Kadirvelu K. Toxicity assessment of pyriproxyfen in vertebrate model zebrafish embryos (*Danio rerio*): A multi biomarker study. *Aquat Toxicol*. 2018; 196:132–45. Epub 2018/02/07. <https://doi.org/10.1016/j.aquatox.2018.01.010> PMID: 29407799.
 23. Cassar S, Breidenbach L, Olson A, Huang X, Britton H, Woody C, et al. Measuring drug absorption improves interpretation of behavioral responses in a larval zebrafish locomotor assay for predicting seizure liability. *J Pharmacol Toxicol Methods*. 2017; 88(Pt 1):56–63. Epub 2017/07/18. <https://doi.org/10.1016/j.vascn.2017.07.002> PMID: 28712933.
 24. Kimmel CB, Ballard WW, Kimmel SR, Ullmann B, Schilling TF. Stages of embryonic development of the zebrafish. *Dev Dyn*. 1995; 203(3):253–310. Epub 1995/07/01. <https://doi.org/10.1002/aja.1002030302> PMID: 8589427.
 25. Ding Y, Lei L, Lai C, Tang Z. Tau Protein and Zebrafish Models for Tau-Induced Neurodegeneration. *J Alzheimers Dis*. 2019; 69(2):339–53. Epub 2019/04/23. <https://doi.org/10.3233/JAD-180917> PMID: 31006683.
 26. Bhattarai P, Cosacak MI, Mashkaryan V, Demir S, Popova SD, Govindarajan N, et al. Neuron-glia interaction through Serotonin-BDNF-NGFR axis enables regenerative neurogenesis in Alzheimer's model of adult zebrafish brain. *PLoS biology*. 2020; 18(1):e3000585. Epub 2020/01/07. <https://doi.org/10.1371/journal.pbio.3000585> PMID: 31905199; PubMed Central PMCID: PMC6964913.
 27. Shenoy A, Banerjee M, Upadhyay A, Bagwe-Parab S, Kaur G. The Brilliance of the Zebrafish Model: Perception on Behavior and Alzheimer's Disease. *Front Behav Neurosci*. 2022; 16:861155. Epub 2022/07/01. <https://doi.org/10.3389/fnbeh.2022.861155> PMID: 35769627; PubMed Central PMCID: PMC9234549.
 28. Rohn TT, Beck JD, Galla SJ, Isho NF, Pollock TB, Suresh T, et al. Fragmentation of Apolipoprotein E4 is Required for Differential Expression of Inflammation and Activation Related Genes in Microglia Cells. *Int J Neurodegener Dis*. 2021; 4(1). Epub 2021/10/26. <https://doi.org/10.23937/2643-4539/1710020> PMID: 34693295; PubMed Central PMCID: PMC8529910.
 29. Peri F, Nusslein-Volhard C. Live imaging of neuronal degradation by microglia reveals a role for v0-ATPase a1 in phagosomal fusion in vivo. *Cell*. 2008; 133(5):916–27. Epub 2008/05/31. <https://doi.org/10.1016/j.cell.2008.04.037> PMID: 18510934.
 30. Gusel'nikova VV, Korzhevskiy DE. NeuN As a Neuronal Nuclear Antigen and Neuron Differentiation Marker. *Acta Naturae*. 2015; 7(2):42–7. Epub 2015/06/19. PMID: 26085943; PubMed Central PMCID: PMC4463411.
 31. Chen M, Martins RN, Lardelli M. Complex splicing and neural expression of duplicated tau genes in zebrafish embryos. *J Alzheimers Dis*. 2009; 18(2):305–17. Epub 2009/07/09. <https://doi.org/10.3233/JAD-2009-1145> PMID: 19584432.
 32. Cantrelle FX, Loyens A, Trivelli X, Reimann O, Despres C, Gandhi NS, et al. Phosphorylation and O-GlcNAcylation of the PHF-1 Epitope of Tau Protein Induce Local Conformational Changes of the C-Terminus and Modulate Tau Self-Assembly Into Fibrillar Aggregates. *Front Mol Neurosci*. 2021; 14:661368. Epub 2021/07/06. <https://doi.org/10.3389/fnmol.2021.661368> PMID: 34220449; PubMed Central PMCID: PMC8249575.
 33. Rohn TT. Proteolytic cleavage of apolipoprotein E4 as the keystone for the heightened risk associated with Alzheimer's disease. *International journal of molecular sciences*. 2013; 14(7):14908–22. Epub 2013/07/23. <https://doi.org/10.3390/ijms140714908> PMID: 23867607; PubMed Central PMCID: PMC3742279.
 34. Dafnis I, Stratikos E, Tzinia A, Tsilibary EC, Zannis VI, Chroni A. An apolipoprotein E4 fragment can promote intracellular accumulation of amyloid peptide beta 42. *J Neurochem*. 2010; 115(4):873–84. <https://doi.org/10.1111/j.1471-4159.2010.06756.x> PMID: 20412390.
 35. Dafnis I, Tzinia AK, Tsilibary EC, Zannis VI, Chroni A. An apolipoprotein E4 fragment affects matrix metalloproteinase 9, tissue inhibitor of metalloproteinase 1 and cytokine levels in brain cell lines. *Neuroscience*. 2012; 210:21–32. Epub 2012/03/27. <https://doi.org/10.1016/j.neuroscience.2012.03.013> PMID: 22445724; PubMed Central PMCID: PMC3358542.

36. Zhou W, Scott SA, Shelton SB, Crutcher KA. Cathepsin D-mediated proteolysis of apolipoprotein E: possible role in Alzheimer's disease. *Neuroscience*. 2006; 143(3):689–701. <https://doi.org/10.1016/j.neuroscience.2006.08.019> PMID: 16997486.
37. Tolar M, Marques MA, Harmony JA, Crutcher KA. Neurotoxicity of the 22 kDa thrombin-cleavage fragment of apolipoprotein E and related synthetic peptides is receptor-mediated. *J Neurosci*. 1997; 17(15):5678–86. <https://doi.org/10.1523/JNEUROSCI.17-15-05678.1997> PMID: 9221767.
38. Mueller T, Wullmann MF. An evolutionary interpretation of teleostean forebrain anatomy. *Brain Behav Evol*. 2009; 74(1):30–42. Epub 2009/09/05. <https://doi.org/10.1159/000229011> PMID: 19729894.
39. Rink E, Wullmann MF. Connections of the ventral telencephalon (subpallium) in the zebrafish (*Danio rerio*). *Brain Res*. 2004; 1011(2):206–20. Epub 2004/05/26. <https://doi.org/10.1016/j.brainres.2004.03.027> PMID: 15157807.
40. Mueller T, Vernier P, Wullmann MF. The adult central nervous cholinergic system of a neurogenetic model animal, the zebrafish *Danio rerio*. *Brain Res*. 2004; 1011(2):156–69. Epub 2004/05/26. <https://doi.org/10.1016/j.brainres.2004.02.073> PMID: 15157802.
41. Valente A, Huang KH, Portugues R, Engert F. Ontogeny of classical and operant learning behaviors in zebrafish. *Learn Mem*. 2012; 19(4):170–7. Epub 2012/03/22. <https://doi.org/10.1101/lm.025668.112> PMID: 22434824; PubMed Central PMCID: PMC3312620.
42. Low SE, Ryan J, Sprague SM, Hirata H, Cui WW, Zhou W, et al. touche Is required for touch-evoked generator potentials within vertebrate sensory neurons. *J Neurosci*. 2010; 30(28):9359–67. Epub 2010/07/16. <https://doi.org/10.1523/JNEUROSCI.1639-10.2010> PMID: 20631165; PubMed Central PMCID: PMC2921932.
43. Arganda S, Perez-Escudero A, de Polavieja GG. A common rule for decision making in animal collectives across species. *Proc Natl Acad Sci U S A*. 2012; 109(50):20508–13. Epub 2012/12/01. <https://doi.org/10.1073/pnas.1210664109> PMID: 23197836; PubMed Central PMCID: PMC3528575.
44. Nery LR, Eltz NS, Hackman C, Fonseca R, Altenhofen S, Guerra HN, et al. Brain intraventricular injection of amyloid-beta in zebrafish embryo impairs cognition and increases tau phosphorylation, effects reversed by lithium. *PLoS One*. 2014; 9(9):e105862. Epub 2014/09/05. <https://doi.org/10.1371/journal.pone.0105862> PMID: 25187954; PubMed Central PMCID: PMC4154875.
45. Paquet D, Schmid B, Haass C. Transgenic zebrafish as a novel animal model to study tauopathies and other neurodegenerative disorders in vivo. *Neurodegener Dis*. 2010; 7(1–3):99–102. Epub 2010/02/23. <https://doi.org/10.1159/000285515> PMID: 20173336.
46. Lahoz C, Schaefer EJ, Cupples LA, Wilson PW, Levy D, Osgood D, et al. Apolipoprotein E genotype and cardiovascular disease in the Framingham Heart Study. *Atherosclerosis*. 2001; 154(3):529–37. Epub 2001/03/21. [https://doi.org/10.1016/s0021-9150\(00\)00570-0](https://doi.org/10.1016/s0021-9150(00)00570-0) PMID: 11257253.
47. Legradi J, el Abdellaoui N, van Pomeran M, Legler J. Comparability of behavioural assays using zebrafish larvae to assess neurotoxicity. *Environ Sci Pollut Res Int*. 2015; 22(21):16277–89. Epub 2014/11/18. <https://doi.org/10.1007/s11356-014-3805-8> PMID: 25399529.
48. Saint-Amant L, Drapeau P. Time course of the development of motor behaviors in the zebrafish embryo. *J Neurobiol*. 1998; 37(4):622–32. Epub 1998/12/19. [https://doi.org/10.1002/\(sici\)1097-4695\(199812\)37:4<622::aid-neu10>3.0.co;2-s](https://doi.org/10.1002/(sici)1097-4695(199812)37:4<622::aid-neu10>3.0.co;2-s) PMID: 9858263.
49. Saint-Amant L, Drapeau P. Synchronization of an embryonic network of identified spinal interneurons solely by electrical coupling. *Neuron*. 2001; 31(6):1035–46. Epub 2001/10/03. [https://doi.org/10.1016/s0896-6273\(01\)00416-0](https://doi.org/10.1016/s0896-6273(01)00416-0) PMID: 11580902.
50. Eaton RC, Farley RD, Kimmel CB, Schabtach E. Functional development in the Mauthner cell system of embryos and larvae of the zebra fish. *J Neurobiol*. 1977; 8(2):151–72. Epub 1977/03/01. <https://doi.org/10.1002/neu.480080207> PMID: 856948.
51. Liu KS, Fetcho JR. Laser ablations reveal functional relationships of segmental hindbrain neurons in zebrafish. *Neuron*. 1999; 23(2):325–35. Epub 1999/07/10. [https://doi.org/10.1016/s0896-6273\(00\)80783-7](https://doi.org/10.1016/s0896-6273(00)80783-7) PMID: 10399938.
52. Saint-Amant L, Drapeau P. Motoneuron activity patterns related to the earliest behavior of the zebrafish embryo. *J Neurosci*. 2000; 20(11):3964–72. Epub 2000/05/20. <https://doi.org/10.1523/JNEUROSCI.20-11-03964.2000> PMID: 10818131; PubMed Central PMCID: PMC6772631.
53. Lin YT, Seo J, Gao F, Feldman HM, Wen HL, Penney J, et al. APOE4 Causes Widespread Molecular and Cellular Alterations Associated with Alzheimer's Disease Phenotypes in Human iPSC-Derived Brain Cell Types. *Neuron*. 2018; 98(6):1294. Epub 2018/06/29. <https://doi.org/10.1016/j.neuron.2018.06.011> PMID: 29953873; PubMed Central PMCID: PMC6048952.
54. Forner S, Baglietto-Vargas D, Martini AC, Trujillo-Estrada L, LaFerla FM. Synaptic Impairment in Alzheimer's Disease: A Dysregulated Symphony. *Trends Neurosci*. 2017; 40(6):347–57. Epub 2017/05/13. <https://doi.org/10.1016/j.tins.2017.04.002> PMID: 28494972.

55. Kowall NW, Kosik KS. Axonal disruption and aberrant localization of tau protein characterize the neuropil pathology of Alzheimer's disease. *Ann Neurol*. 1987; 22(5):639–43. Epub 1987/11/01. <https://doi.org/10.1002/ana.410220514> PMID: 3122646.
56. Lefebvre JL, Ono F, Puglielli C, Seidner G, Franzini-Armstrong C, Brehm P, et al. Increased neuromuscular activity causes axonal defects and muscular degeneration. *Development*. 2004; 131(11):2605–18. Epub 2004/05/07. <https://doi.org/10.1242/dev.01123> PMID: 15128655.
57. Safieh M, Korczyn AD, Michaelson DM. ApoE4: an emerging therapeutic target for Alzheimer's disease. *BMC Med*. 2019; 17(1):64. Epub 2019/03/21. <https://doi.org/10.1186/s12916-019-1299-4> PMID: 30890171; PubMed Central PMCID: PMC6425600.